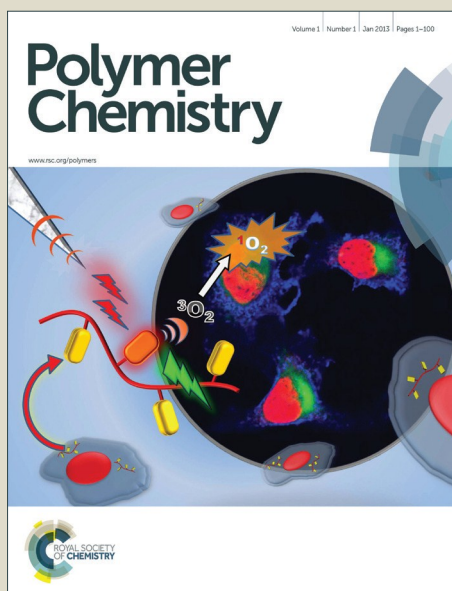


# Polymer Chemistry

Accepted Manuscript



This is an *Accepted Manuscript*, which has been through the Royal Society of Chemistry peer review process and has been accepted for publication.

*Accepted Manuscripts* are published online shortly after acceptance, before technical editing, formatting and proof reading. Using this free service, authors can make their results available to the community, in citable form, before we publish the edited article. We will replace this *Accepted Manuscript* with the edited and formatted *Advance Article* as soon as it is available.

You can find more information about *Accepted Manuscripts* in the [Information for Authors](#).

Please note that technical editing may introduce minor changes to the text and/or graphics, which may alter content. The journal's standard [Terms & Conditions](#) and the [Ethical guidelines](#) still apply. In no event shall the Royal Society of Chemistry be held responsible for any errors or omissions in this *Accepted Manuscript* or any consequences arising from the use of any information it contains.

## ARTICLE

# Borinic Acid Block Copolymer: New Building Blocks for Supramolecular Assembly and Sensory Applications

Cite this: DOI: 10.1039/x0xx00000x

Received 00th January 2012,  
Accepted 00th January 2012

DOI: 10.1039/x0xx00000x

www.rsc.org/

Fei Cheng,<sup>a†</sup> Wen-Ming Wan,<sup>a,b‡\*</sup> Yan Zhou,<sup>b</sup> Xiao-Li Sun,<sup>c</sup> Edward M. Bonder,<sup>d</sup>  
Frieder Jäkle<sup>a\*</sup>

**ABSTRACT:** Borinic acid block copolymers have been prepared by reversible addition-fragmentation chain transfer (RAFT) polymerization and investigated as “smart materials” in sensory applications. Taking advantage of the hydrogen bond donating ability of the borinic acid groups, supramolecular aggregates of PNIPAM-*b*-PBA were generated by complexation with P<sub>4</sub>VP. The P<sub>4</sub>VP complex showed greatly improved fluoride ion detection efficiency relative to the PBA polymer by itself. The block copolymer PS-*b*-PBA was processed into porous films with tunable pore size by drop-casting from THF in the presence of trace amounts of water. A microporous polymer film that was deposited on an electrode was utilized as a biosensor for acetylthiocholine chloride detection after immobilization of acetylcholine esterase.

## Introduction

Boron-containing polymeric materials have gained some prominence as new functional materials in recent years.<sup>1</sup> For example, luminescent triarylborane-functionalized polymers have been explored in sensing applications, taking advantage of reversible Lewis acid-base interactions with anions and neutral Lewis bases that lead to changes in the absorption and emission profiles.<sup>2</sup> The high affinity and reversible binding of diols and polyols of boronic acid and boroxole-functionalized polymers has been applied for sugar sensing and other biomedical applications.<sup>1i, 3</sup> Of particular note is the development of new advanced polymeric materials that are able to not only bind to sugars at physiological pH, but also take advantage of block copolymer self-assembly principles to provide multi-stimulus responsive behavior (A-C, Chart 1).<sup>3b, 3d, 3j</sup>

Compared to boronic acid polymers, borinic acid-functionalized polymers are far less well-developed, in spite of their facile synthesis, enhanced Lewis acidity and excellent substrate binding capability.<sup>4</sup> Recently, we reported that poly(styrylphenyl(tri-*iso*-propylphenyl)-borinic acid) (PBA, Chart 1) shows interesting thermo-responsive properties. The upper critical solution temperature (UCST) of PBA in DMSO increases linearly as the amount of added water increases from 0 to 2.5% (v/v), making it continuously tunable over a wide temperature range from 20 to 100 °C.<sup>5</sup> However, other potential applications that take advantage of this new class of polymers as building blocks for supramolecular assembly and “smart” materials have yet to be explored. The development of block

copolymers with borinic acid functional groups in well-defined positions is an important step toward that goal.

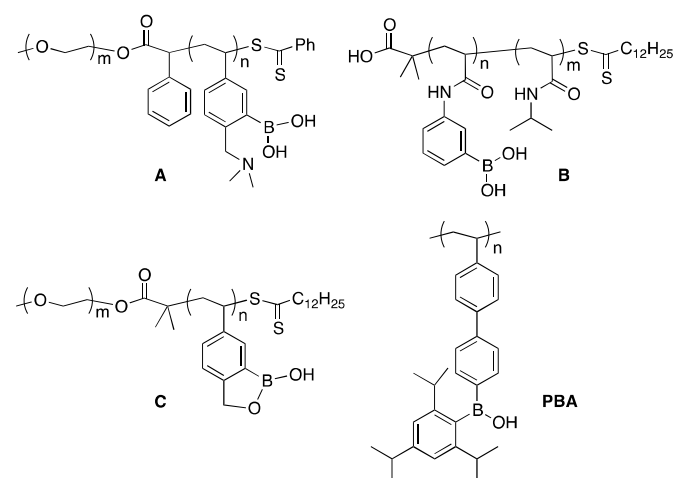


**Chart 1.** Examples of multi-responsive boronic acid block copolymers (A-C) and the structure of borinic acid polymer PBA.

Herein, we describe the synthesis and properties of the first borinic acid block copolymers. We report on the self-assembly behavior of a block copolymer with PNIPAM and its interactions with P<sub>4</sub>VP as a poly-Lewis base and hydrogen bond acceptor. The utility of the resulting composite in fluoride anion detection is examined. In addition, the immobilization of acetylcholine esterase on a porous film derived from a PS block copolymer and its application as a biosensor are demonstrated.

## Experimental

**Materials.** 1,4-Dioxane and THF were distilled from Na/benzophenone prior to use. The azobisisobutyronitrile (AIBN) initiator was recrystallized in methanol. Styrene was purified by passing it through a neutral alumina column and then distilled under reduced pressure. N-isopropyl acrylamide (NIPAM) was purified by recrystallization in a hexanes/benzene mixture. All other solvents and chemicals were used without further purification. The molecular chain transfer agents (CTA),<sup>6</sup> the PS-CTA<sup>7</sup> ( $M_{n, GPC-RI} = 8130$  g/mol,  $D = 1.16$ ,  $M_{n, GPC-MALLS} = 9500$  g/mol), the borinic acid monomer BA,<sup>5</sup> and the homopolymer PBA<sup>5</sup> were synthesized according to literature procedures.

**Synthesis of PNIPAM-CTA.** The PNIPAM-CTA was synthesized in analogy to a literature procedure.<sup>7</sup> Into a Schlenk tube were loaded NIPAM (9.04 g, 80.0 mmol), benzyl dithiobenzoate (BDTB) (200 mg, 0.80 mmol), AIBN (26.2 mg, 0.16 mmol), and 20.0 mL of dioxane ([NIPAM]/[CTA]/[AIBN] = 100/1/0.2). After 3 freeze-pump-thaw cycles, the tube was immersed in a 70 °C oil bath and the mixture stirred for 24 h. The reaction was terminated by placing the tube in liquid nitrogen. The polymer was precipitated in a 10-fold volume of diethyl ether and then reprecipitated 2 more times from THF into diethyl ether. After drying in high vacuum, 3.06 g of PNIPAM-CTA were obtained as a pink powder (32% conversion). GPC-RI (DMF with 0.2% Bu<sub>4</sub>NBr):  $M_{n, GPC-RI} = 9630$  g/mol,  $D = 1.09$ ,  $m_{GPC} = 82$ .

**Synthesis of PNIPAM-*b*-PBA.** PNIPAM-CTA (72 mg, 7.5 μmol based on GPC-RI), BA monomer (220 mg, 0.536 mmol), and AIBN (0.74 mg, 4.5 μmol) were dissolved in 2.0 mL of 1,4-dioxane in a Schlenk tube ([BA]/[PNIPAM-CTA]/[AIBN] = 72/1/0.6). After 3 freeze-pump-thaw cycles, the Schlenk tube was immersed in an 80 °C oil bath and the mixture stirred for 5 h. The polymerization was quenched by immersing the tube in liquid nitrogen. The polymer was precipitated in a 10-fold volume of cold hexanes and then reprecipitated 2 more times from THF into cold hexanes. After drying in high vacuum, the product was obtained as a light pink powder (185 mg, 51% BA monomer conversion). <sup>1</sup>H NMR (499.895 MHz, CDCl<sub>3</sub>): δ = 7.8, 7.5, 7.2~6.2 (overlapped aromatic and amide protons), 5.9 (B-OH), 4.0 (NHCHMe<sub>2</sub>), 2.9 (*para*-CHMe<sub>2</sub>), 2.7 (*ortho*-CHMe<sub>2</sub>), 2.4~1.4 (overlapped, backbone H), 1.3 (*para*-CHMe<sub>2</sub>), 1.2 (*ortho*-CHMe<sub>2</sub> and NHCHMe<sub>2</sub>). <sup>11</sup>B NMR (160.386 MHz, CDCl<sub>3</sub>) δ = 43. <sup>13</sup>C NMR (125.698 MHz, CDCl<sub>3</sub>): δ = 174.3 (C=O), 150.8, 149.4, 146.4~144.4 (broad), 144.0, 138.1, 136.0, 135.7, 128.3 (broad), 126.9 (broad), 126.2, 120.5, 42.7, 41.5, 35.0, 34.5, 24.8 (broad), 24.2, 22.8. GPC-RI (DMF with 0.2% Bu<sub>4</sub>NBr):  $M_n = 27020$  g/mol,  $D = 1.26$ ;  $m_{GPC} = 82$ ;  $n_{GPC} = 42$ . The ratio *m/n* is 1.8 based on <sup>1</sup>H NMR integration (using peaks at 4.0 ppm and 2.9 ppm as reference).

**Synthesis of PS-*b*-PBA.** PS-CTA (36 mg, 10 μmol based on GPC-RI), BA monomer (164 mg, 0.40 mmol), and AIBN (0.2 mg, 1.0 μmol) were dissolved in 0.3 mL of THF in a Schlenk tube ([BA]/[PS-CTA]/[AIBN] = 40/1/0.1). After 3 freeze-pump-thaw cycles, the Schlenk tube was immersed in an

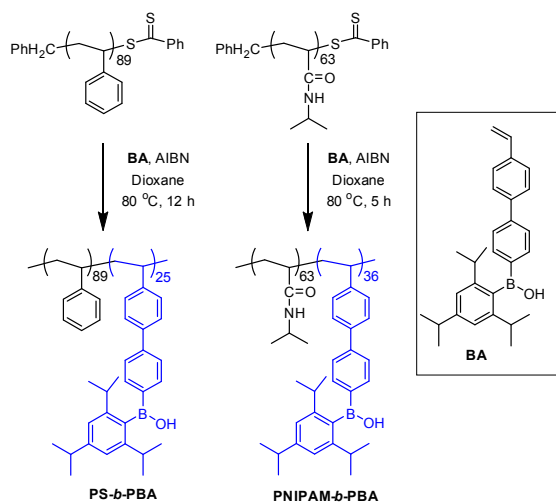
80 °C oil bath and the mixture stirred for 12 h. The polymerization was quenched by placing the tube in liquid nitrogen. The mixture was diluted with 3 mL of THF, the polymer precipitated in a 10-fold volume of MeOH/H<sub>2</sub>O (5/1) and then reprecipitated 2 more times from THF into MeOH/H<sub>2</sub>O (5/1). After drying in high vacuum, the product was obtained as a light pink powder (124 mg, 54% BA monomer conversion). <sup>1</sup>H NMR (499.895 MHz, CDCl<sub>3</sub>): δ = 7.8, 7.5, 7.2~6.2 (overlapped aromatic protons), 5.8 (B-OH), 2.9 (*para*-CHMe<sub>2</sub>), 2.7 (*ortho*-CHMe<sub>2</sub>), 2.3~1.3 (overlapped, backbone protons), 1.3 (*para*-CHMe<sub>2</sub>), 1.2 (*ortho*-CHMe<sub>2</sub>). <sup>11</sup>B NMR (160.386 MHz, CDCl<sub>3</sub>) δ = 42 (*w*<sub>1/2</sub> = 2900 Hz). <sup>13</sup>C NMR (125.698 MHz, CDCl<sub>3</sub>): δ = 150.3, 149.2, 145.5 (broad), 143.6, 136.8, 136.6, 136.0, 133.6, 129.0~127.3 (overlapped), 126.8 (broad), 126.4~125.4 (overlapped), 120.3, 46-40 (PS backbone), 35.1, 34.5, 24.8, 24.3. GPC-RI (THF):  $M_n = 12200$  g/mol,  $D = 1.29$ ;  $m_{GPC} = 89$ ;  $n_{GPC} = 27$ . The ratio *m/n* is 3.6 based on <sup>1</sup>H NMR integration (using peaks at 6.8-6.2 ppm and 2.9 ppm as reference).

**Porous Film Formation of PS-*b*-PBA.** A solution of block copolymer PS-*b*-PBA was prepared in anhydrous THF (1 mg/mL) and kept at room temperature overnight. To the polymer solution was then added the desired amount of H<sub>2</sub>O with stirring. A film of the polymer was generated by drop casting 10 μL of PS-*b*-PBA solution on a mica plate, followed by rapid evaporation under N<sub>2</sub> flow. The morphologies were characterized by AFM in the tapping mode.

**Fabrication of Biosensor based on AChE/PS-*b*-PBA-Coated Electrode.** 10 μL of PS-*b*-PBA solution (1 mg/mL, 3% of H<sub>2</sub>O in THF (v/v)) were added dropwise on an electrode surface, followed by rapid evaporation under N<sub>2</sub> flow. The electrode was kept as is for about 5 min at room temperature. Then 10 μL of PBS buffer (pH = 7.0, 0.1 M) containing 0.01 U of acetylcholinesterase (AChE) enzyme solution were spread on the modified electrode surface and the electrode was kept at 4 °C overnight. Finally, the electrode was washed twice with PBS buffer and then used further for acetylthiocholine chloride (ASChCl) detection.

## Results and discussion

**Synthesis of Borinic Acid Block Copolymers.** The borinic acid block copolymers PS-*b*-PBA and PNIPAM-*b*-PBA were synthesized by RAFT polymerization of BA in the presence of PS ([BA]/[PS-CTA]/[AIBN] = 40/1/0.1) and PNIPAM ([BA]/[PNIPAM-CTA]/[AIBN] = 71.5/1/0.6) as macro-CTAs (Scheme 1). The resulting block copolymers were isolated as light pink powdery solids after reprecipitation into MeOH/H<sub>2</sub>O mixture (PS-*b*-PBA) or cold hexanes (PNIPAM-*b*-PBA). The products were examined by GPC-RI analysis. Single symmetric peaks in the GPC traces are consistent with a well-controlled polymerization (Figure 1). The molecular weights of the block copolymers are significantly higher than those of the macro-



Scheme 1. Synthesis of borinic acid block copolymers

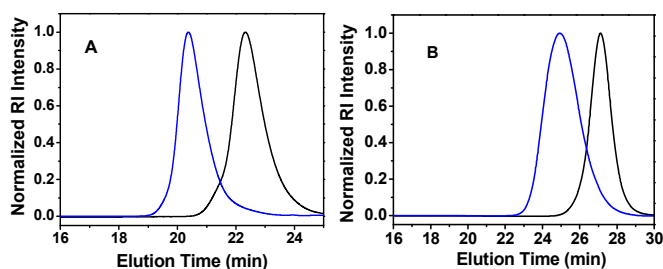
Figure 1. GPC overlays. (A) PS-CTA (black) and PS-*b*-PBA (blue) in THF at 1 mL min<sup>-1</sup>; (B) PNIPAM-CTA (black) and PNIPAM-*b*-PBA (blue) in DMF with 0.2% (w/w) of Bu<sub>4</sub>NBr at 0.5 mL min<sup>-1</sup>.

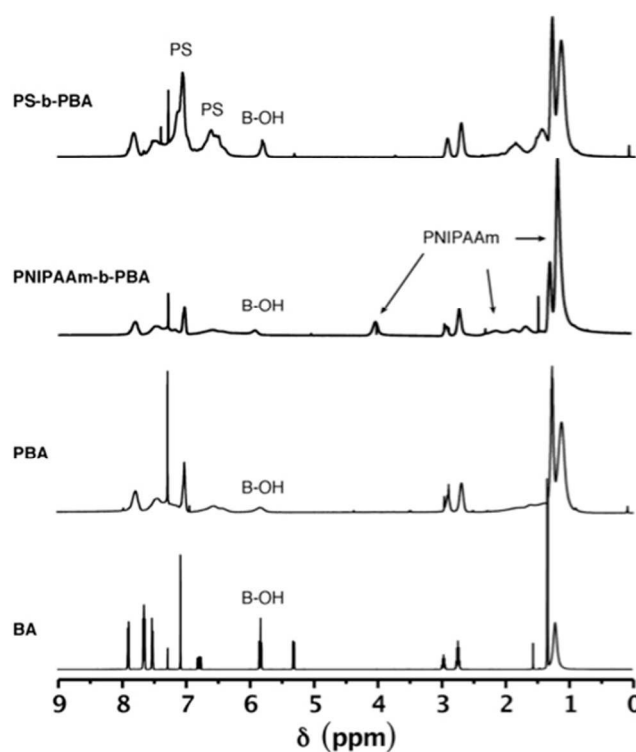
Table 1. Comparison of polymer molecular weight data

Polymer <sup>a</sup>	$M_n$ , GPC	$D_{GPC}$	$M_n$ , MALLS	$m, n$ GPC <sup>b</sup>	$m, n$ NMR <sup>c</sup>
PBA <sub>n</sub> <sup>d</sup>	38500	1.26	<sup>e</sup>	94	86
PS <sub>m</sub> -CTA	8130	1.16	9470	89	89
PS <sub>m</sub> - <i>b</i> -PBA <sub>n</sub>	16880	1.28	20400	89, 27	89, 25
PNIPAM <sub>m</sub> -CTA	9630	1.09	<sup>e</sup>	82	63
PNIPAM <sub>m</sub> - <i>b</i> -PBA <sub>n</sub>	27020	1.26	<sup>e</sup>	82, 42	63, 36

<sup>a</sup>  $m$  and  $n$  refer to the degree of polymerization of the first and second block, respectively. <sup>b</sup> Determined by GPC-MALLS (PS<sub>m</sub>-*b*-PBA<sub>n</sub>) or GPC-RI (PNIPAM<sub>m</sub>-*b*-PBA<sub>n</sub>). <sup>c</sup> Based on <sup>1</sup>H NMR integration (6.8–6.2 and 2.9 ppm for PS<sub>m</sub>-*b*-PBA<sub>n</sub>, 4.0 and 2.9 ppm for PNIPAM<sub>m</sub>-*b*-PBA<sub>n</sub>). <sup>d</sup> Reference 5. <sup>e</sup> Not measured.

CTA precursors and consistent with the calculated molecular weights based on the product yield, confirming successful chain extension. The dispersities ( $D$ ) of the homopolymer and block copolymers are quite narrow.

The well-defined structure of the polymers was further confirmed by <sup>1</sup>H, <sup>11</sup>B and <sup>13</sup>C NMR spectroscopy (Figure 2, Figure S1-2). The <sup>11</sup>B NMR signals of the block copolymers

Figure 2. Comparison of the <sup>1</sup>H NMR spectra of monomer BA, homopolymer PBA, and block copolymers PS-*b*-PBA and PNIPAM-*b*-PBA in CDCl<sub>3</sub>

(~43 ppm) appear at a similar chemical shift as the homopolymer and they are all slightly upfield shifted relative to the monomer (49 ppm). In the <sup>1</sup>H NMR spectra, the borinic acid groups are found as broad signals at ca. 5.8 ppm for both the monomer and polymers. For PS-*b*-PBA, the degree of polymerization of the PBA block was estimated by comparing the integrals of the isopropyl moieties at 2.9 ppm with the PS aromatic signals at 6.8–6.2 ppm (minus the PBA contribution) and for PNIPAM-*b*-PBA by comparison of the C-H signals at 4.0 and 2.9 ppm. The results are consistent with the GPC data (Table 1). We conclude that well-defined homo and block copolymers with fairly high molecular weights and narrow distribution were successfully obtained.

**Photophysical Properties of Borinic Acid Polymers.** The polymers show an intense absorption at ca. 280 nm and are strongly luminescent in THF solution. In comparison to the monomer BA ( $\lambda_F = 345$  nm,  $\Phi_F = 0.82$ ), the absorptions of the polymers are slightly blue shifted and the emissions are broadened (Figure S3-5). The quantum yields of  $\Phi_F \sim 0.37$  are lower than that for the monomer, possibly because of bimolecular quenching of neighboring borane chromophores along the polymer chain. The photophysical properties are summarized in Table 2.

**Table 2.** Photophysical properties of monomer BA and corresponding polymers in THF

Sample	$\lambda_{\text{abs}}$ (nm)	$\epsilon$ (cm <sup>2</sup> M <sup>-1</sup> )	$\lambda_{\text{em}}$ (nm) <sup>a</sup>	$\Phi_{\text{f}}$
BA <sup>b</sup>	294	26290	345	0.82
PBA <sup>b</sup>	283	28100 <sup>c</sup>	~330-360	0.37
PS- <i>b</i> -PBA	280	28080 <sup>c,d</sup>	~330-360	0.36
PNIPAM- <i>b</i> -PBA	282	29750 <sup>c,d</sup>	~330-360	0.38

<sup>a</sup> All samples were excited at the corresponding  $\lambda_{\text{abs}}$ . <sup>b</sup> Reference 5. <sup>c</sup> Molar extinction coefficient for the BA repeat unit. <sup>d</sup> Estimated according to the block ratio derived from the <sup>1</sup>H NMR integration.

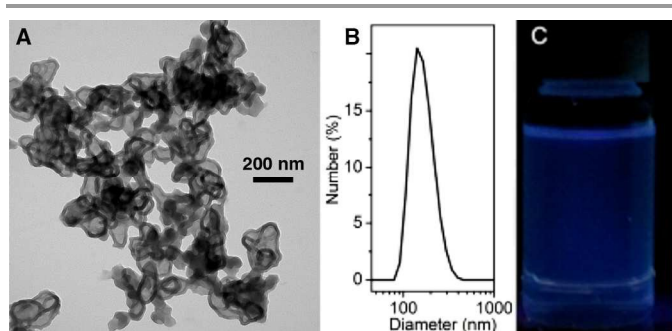


**Figure 3.** (A) TEM micrograph and (B) size distribution by DLS of PNIPAM-*b*-PBA vesicles formed by self-assembly in water. (C) Photograph of PNIPAM-*b*-PBA vesicles under UV-irradiation (365 nm hand-held UV lamp).

**Borinic Acid Polymers as Building Blocks for Supramolecular Self-Assembly and Anion Detection.** We first examined the self-assembly behavior of the amphiphilic block copolymer PNIPMA-*b*-PBA in water, where the presence of the hydrophobic polystyrene-like backbone of PBA and hydrophilic PNIPAM segment are expected to result in aggregation. The morphology of the resulting aggregates was examined by TEM and DLS. As shown in Figure 3, vesicles with a diameter of about 200 nm were observed. Due to the softness of the polymeric material, the thin-walled vesicles were broken and fused together on the copper grid. DLS characterization revealed a size of  $\langle D_{\text{h}} \rangle = 173 \pm 57$  nm.

As weak Brønsted acids, borinic acids are also well known to reversibly associate with hydrogen bond acceptors.<sup>8</sup> Similar as in the case of poly(4-hydroxystyrene), which has attracted significant research interest as a building block to nanostructured materials,<sup>9</sup> this behavior provides another opportunity to utilize the borinic acid polymers for luminescent supramolecular nanostructures and could be advantageous in the development of new types of stimuli-responsive or sensory materials. Hence, we investigated the co-assembly of the borinic acid polymers as H-bond donors with poly(4-vinylpyridine) (P4VP,  $M_{\text{n}} = 15200$  Da), a well-known H-bond acceptor.<sup>10</sup> Dichloromethane (DCM) was chosen as a good solvent, in which the PBA (co)polymers as well as P4VP are molecularly dissolved. Upon slow addition of a P4VP solution ([Py] = 5 mM in DCM) into a solution of the respective PBA polymers ([B-OH] = 1.1 mM in DCM) under stirring, features

of opalescence due to polymeric colloids appeared once the pyridine/B-OH molar ratio reached  $\sim 1/10$  (Figure S7). DLS results for the mixtures of PBA/P4VP, PNIPAM-*b*-PBA/P4VP and PS-*b*-PBA/P4VP are summarized in Table 3 and displayed in Figure 4. The observed particle sizes of the P4VP composites are much larger than those of the single polymer chains in DCM, confirming the formation of supramolecular aggregates. These assemblies remain highly luminescent, similar to the PBA homo and block copolymer solutions in the absence of P4VP (Figure S7). The proposed mechanism of the H-bond-induced supramolecular co-assembly, where pyridine moieties act as H-bond acceptors while the borinic acid moieties serve as donors, is illustrated in Figure 5. The H-bond formation causes a solubility change of the PBA-containing polymers, resulting in phase separation of the PBA/P4VP core that is surrounded and stabilized by the PS or PNIPAM block in the shell.

**Table 3.** DLS results for supramolecular micelles with P4VP in DCM.

Sample	Additive	PBA	PS- <i>b</i> -PBA	PNIPAM- <i>b</i> -PBA
$\langle D_{\text{h}} \rangle$	none	2.0±0.2	2.0±0.3	2.4±0.4
$\langle D_{\text{h}} \rangle$	P4VP <sup>a</sup>	531±211	396±156	712±234

<sup>a</sup> For P4VP:  $\langle D_{\text{h}} \rangle = 2.2 \pm 0.3$  nm.

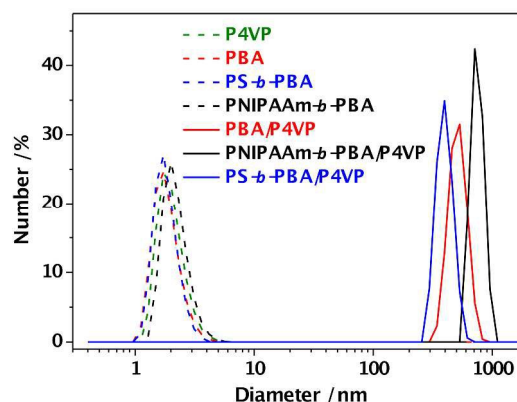


**Figure 4.** DLS size distributions of PBA/P4VP, PNIPAM-*b*-PBA/P4VP and PS-*b*-PBA/P4VP supramolecular micelles, and PBA, PNIPAM-*b*-PBA, PS-*b*-PBA and P4VP single chains in DCM.

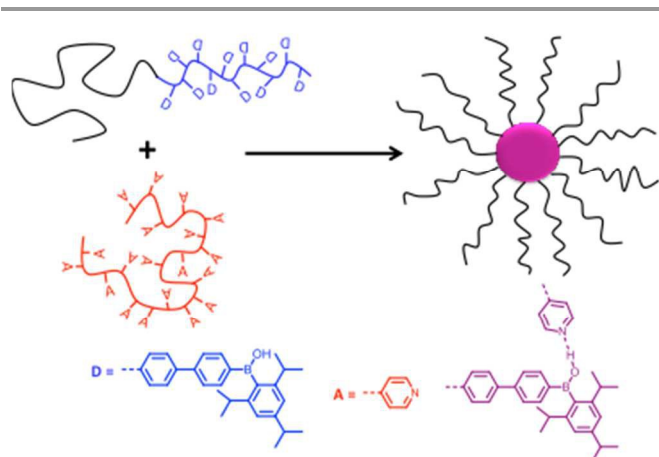


**Figure 5.** Schematic illustration of proposed H-bonding induced supramolecular assembly. D = donor; A = acceptor.

We note that as a Lewis base, pyridine can also form Lewis acid-base complexes with tricoordinate boranes.<sup>1a</sup> To confirm that the supramolecular co-assembly of the PBA polymers and P4VP results from H-bonding rather than Lewis acid-base interactions, we acquired the <sup>1</sup>H and <sup>11</sup>B NMR spectra of a mixture of the borinic acid monomer BA and 4-*t*-butylpyridine in CDCl<sub>3</sub> (Figure S8). The proton NMR signal of the –OH group completely disappeared, which is a sign of H-bonding. Meanwhile, the mixture showed an identical <sup>11</sup>B NMR signal as the monomer by itself, indicating the absence of significant Lewis acid/base interactions. We attribute this to the steric hindrance of the tri-*iso*-propylphenyl substituent and electron-donating nature of the OH group, both of which diminish the borane Lewis acidity.

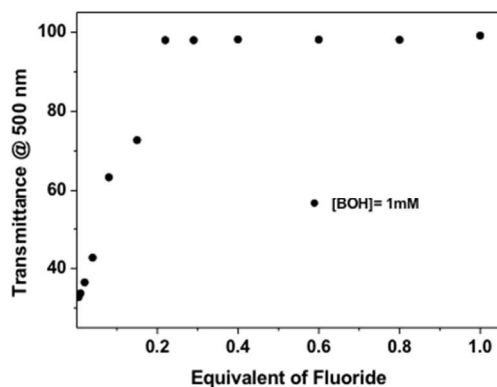


**Figure 6.** Changes in transmittance of a PNIPAM-*b*-PBA/P4VP solution in DCM ([B-OH] = 1 mM), upon addition of TBAF in DCM ([TBAF] = 10 mM).

Although pyridine binding to the borinic acid moieties via B-N bond formation is not favorable in PBA, fluoride as a smaller and more powerful Lewis base should be able to attack the boron atoms. The ability of organoboranes and boronic esters to form complexes with fluoride and other small anions has been widely exploited for the development of fluoride anion sensors.<sup>1e, 2a-h, 11</sup> Indeed, for the borinic acid monomer BA, addition of a 5-fold excess of tetrabutylammonium fluoride

(TBAF) resulted in complete conversion of R<sub>2</sub>BOH to the ionic R<sub>2</sub>BF<sub>2</sub><sup>-</sup> moiety (Figure S10). Meanwhile, for polymer PBA in DMSO ca. 10 equivs of TBAF were required to induce an easily detectable change from a turbid to a clear solution. In comparison, much improved fluoride ion sensitivity was discovered for the supramolecular complex of PNIPAM-*b*-PBA with P4VP, as shown in Figure 6. The block copolymer complex was used since it displays better stability than the homopolymer complex, due to the stabilizing effect of the PNIPAM block. A solution of the PNIPAM-*b*-PBA/P4VP complex showed a transmittance of ~33% in DCM before fluoride ion addition. Upon titration with TBAF, the solution became gradually more transparent with an increase in transmittance from 42% at 0.04, 73% at 0.12, to 98% at 0.22 equiv TBAF. The low ratio of F<sup>-</sup>/B = 0.22 required to achieve this visual change indicates that the sensitivity of fluoride ion detection is greatly enhanced by using the block copolymer composite of PNIPAM-*b*-PBA/P4VP. The greater sensitivity is attributed primarily to the more dramatic solubility changes upon partial conversion of B(OH) to BF<sub>2</sub><sup>-</sup> units in the block copolymer complex. Enhanced binding in the presence of P4VP due to electrostatic effects of quaternized pyridinium moieties that favor borate anion formation may also play a role.<sup>2h</sup>

**Microporous Films of Borinic Acid Block Copolymer as Biosensors.** The previously described anion binding experiments were performed in solution. To explore the utility of borinic acid polymer films for sensing applications, we decided to investigate the film forming properties of the block copolymer PS-*b*-PBA. Block copolymers in general have been widely used to fabricate thin films with different nano or sub-micron patterns.<sup>12</sup>

When 10 μL of PS-*b*-PBA solution (1 mg/mL) in THF containing different amounts of H<sub>2</sub>O were drop-cast on mica, AFM characterization revealed the formation of microporous films (Figure 7). The size of the pores increased from 87±22, 135±32, 238±64 to 681±97 nm as the amount of water in the THF solution of PS-*b*-PBA was raised from 0.1%, 0.3%, 1% to 3%. We hypothesize that water droplets are generated during solvent evaporation, which are stabilized by hydrogen bonding to the polymer-attached BOH groups, resulting in formation of

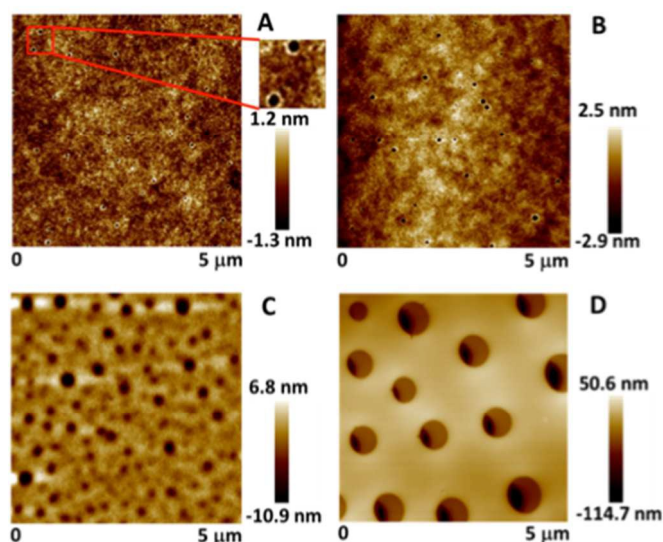
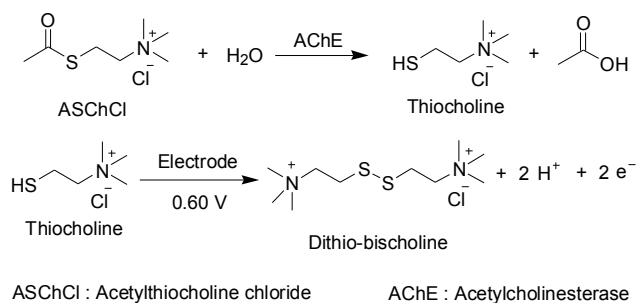


**Figure 7.** AFM micrographs (height) of PS-*b*-PBA block copolymer films formed on mica. [PS-*b*-PBA] = 1 mg/mL. (A) 0.1% H<sub>2</sub>O in THF (v/v); (B) 0.3% H<sub>2</sub>O in THF (v/v); (C) 1% H<sub>2</sub>O in THF (v/v); (D) 3% H<sub>2</sub>O in THF (v/v).

cavities in the polymer film that expose the functional groups. The pore size is determined by the size of the water droplets, which correlates well with the amount of added water. This phenomenon appears to be similar to the formation of honeycomb film structures (so-called breath figures), which are known to develop upon very slow evaporation of solutions of amphiphilic polymers in an environment of controlled humidity.<sup>13</sup> In our case, porous films are formed simply by drop-casting and in the absence of humidity. Only a tiny change in the water content (from 0.1% to 3%) causes a large change in the pore size.

The borinic acid-functionalized polymer films thus generated should be suitable for immobilization of bioactive enzymes containing hydroxyl groups, considering that the BOH groups react with alcohols with formation of borinic esters (Figure S11, S12) and (molecular) diaryl borinic acid compounds have been shown to be bioactive.<sup>4</sup> Using a similar procedure to the one described above, a PS-*b*-PBA film was generated on a working electrode. The film was treated with acetylcholinesterase (AChE) to covalently bind the enzyme to the borinic acid sites, which are expected to be located both at the surface of the film and in the pores, and subsequently rinsed with PBS buffer to remove unbound enzyme. The modified film was then used as a biosensor in the detection of acetylthiocholine chloride (ASChCl) as the substrate. The mechanism of the AChE biosensor is illustrated in Scheme 2, where the electrode serves to detect thiocholine formed after enzyme-catalyzed acetylthiocholine reaction.<sup>14</sup> A clear and repeatable electrical signal is apparent upon addition of ASChCl (20 μM) and the current shows a linear relationship with the ASChCl concentration (Figure 8). The porosity of the polymer film is important as it allows for direct contact to the electrode surface. For a continuous film without the porous structure a poor biosensor response was observed (Figure S13).

Meanwhile, organophosphorus and carbamate pesticides have been widely used in agriculture due to the high efficiency in insect control; these pesticides can inhibit AChE efficiently,<sup>15</sup> suggesting potential for residual pesticides detection as well.



**Scheme 2.** Illustration of electrochemical mechanism of acetylcholinesterase (AChE) biosensor for acetylthiocholine chloride (ASChCl) substrate detection.

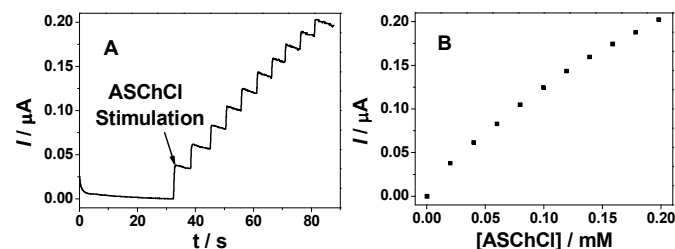


**Figure 8.** Typical response of PBA biosensor in ASChCl detection. (A) Current-time curve upon ASChCl stimulation; (B) Current-[ASChCl] dependence.

## Conclusions

We report the synthesis of well-defined luminescent borinic acid block copolymers by RAFT polymerization. Taking advantage of the hydrogen bond donor property of the borinic acid groups, supramolecular aggregates of the block copolymer PNIPAM-*b*-PBA were generated by complexation with P4VP. We demonstrate that the resulting P4VP complexes show greatly improved fluoride ion detection efficiency relative to the PBA polymer. The block copolymer PS-*b*-PBA was processed into a porous film with tunable pore size by drop-casting a THF solution in the presence of trace amounts of H<sub>2</sub>O. Upon immobilization of acetylcholine esterase, the resulting thin film was applied as an electrochemical biosensor for ASChCl substrate detection with some potential ramifications for organophosphorus and carbamate pesticides detection. Thus, the borinic acid containing polymers hold potential as a new type of “smart” materials in the areas of thermo-responsive, sensory, and supramolecular materials.

## Acknowledgements

Financial support for this work was provided by the National Science Foundation, grants CHE-1112195 and CHE-1308517;

Rutgers University; “the Fundamental Research Funds for the Central Universities” 15CX02028A, 15CX06040A, 15CX02063A and 14CX02154A; China University of Petroleum (East China) starting funding 2014010603, 2014010577 and 2013010008.

## Notes and references

<sup>a</sup> Department of Chemistry, Rutgers University Newark, 73 Warren Street, Newark, NJ 07102, United States.

<sup>b</sup> State Key Laboratory of Heavy Oil Processing and Centre for Bioengineering and Biotechnology, China University of Petroleum (East China), 66 Changjiang West Road, Qingdao Economic Development Zone, Qingdao, Shandong, 266580, People’s Republic of China.

<sup>c</sup> Department of Material Physics and Chemistry, China University of Petroleum (East China), 66 Changjiang West Road, Qingdao Economic Development Zone, Qingdao, Shandong, 266580, People’s Republic of China.

<sup>d</sup> Department of Biological Sciences, Rutgers University-Newark, 195 University Avenue, Newark, NJ 07102, United States.

‡ These authors contributed equally.

\* to whom correspondence should be addressed: wanwenming@upc.edu.cn; fjaekle@rutgers.edu.

Electronic Supplementary Information (ESI) available: Detailed experimental section and supporting data. See DOI: 10.1039/b000000x/

- a) F. Jäkle, *Coord. Chem. Rev.*, 2006, **250**, 1107-1121; b) N. Matsumi and Y. Chujo, *Polym. J.*, 2008, **40**, 77-89; c) K. Severin, *Dalton Trans.*, 2009, 5254-5264; d) A. L. Korich and P. M. Iovine, *Dalton Trans.*, 2010, **39**, 1423-1431; e) F. Jäkle, *Chem. Rev.*, 2010, **110**, 3985-4022; f) A. Nagai and Y. Chujo, *Chem. Lett.*, 2010, **39**, 430-435; g) F. Cheng and F. Jäkle, *Polym. Chem.*, 2011, **2**, 2122-2132; h) E. Sheepwash, V. Krampl, R. Scopelliti, O. Sereda, A. Neels and K. Severin, *Angew. Chem., Int. Ed.*, 2011, **50**, 3034-3037; i) J. N. Cambre and B. S. Sumerlin, *Polymer*, 2011, **52**, 4631-4643; j) A. Doshi and F. Jäkle, in *Comprehensive Inorganic Chemistry II*, eds. J. Reedijk and K. Poepelmeier, Oxford: Elsevier, 2013, vol. 1, pp. 861-891.
- a) M. Miyata and Y. Chujo, *Polym. J.*, 2002, **34**, 967-969; b) A. Sundararaman, M. Victor, R. Varughese and F. Jäkle, *J. Am. Chem. Soc.*, 2005, **127**, 13748-13749; c) K. Parab, K. Venkatasubbaiah and F. Jäkle, *J. Am. Chem. Soc.*, 2006, **128**, 12879-12885; d) H. Li and F. Jäkle, *Angew. Chem. Int. Ed.*, 2009, **48**, 2313-2316; e) H. Kutz, F. Cheng, S. Schwedler, L. Bohling, A. Brockhinke, L. Weber, K. Parab and F. Jäkle, *ACS Macro Lett.*, 2012, **1**, 555-559; f) F. Pammer and F. Jäkle, *Chem. Sci.*, 2012, **3**, 2598-2606; g) A. Rostami and M. S. Taylor, *Macromol. Rapid Comm.*, 2012, **33**, 21-34; h) F. Cheng, E. M. Bonder and F. Jäkle, *J. Am. Chem. Soc.*, 2013, **135**, 17286-17289; i) W. Y. Sung, M. H. Park, J. H. Park, M. Eo, M.-S. Yu, Y. Do and M. H. Lee, *Polymer*, 2012, **53**, 1857-1863.
- a) D. G. Hall, ed., *Boronic Acids: Preparation and Applications in Organic Synthesis and Medicine*, Wiley-VCH Verlag GmbH & Co. KGaA, Weinheim, Germany, 2005; b) D. Roy, J. N. Cambre and B. S. Sumerlin, *Chem. Commun.*, 2009, 2106-2108; c) K. T. Kim, J. J. L. M. Cornelissen, R. J. M. Nolte and J. C. M. van Hest, *Adv. Mater.*, 2009, **21**, 2787-2791; d) K. T. Kim, J. J. L. M. Cornelissen, R. J. M. Nolte and J. C. M. van Hest, *J. Am. Chem. Soc.*, 2009, **131**, 13908-13909; e) S. Li, E. N. Davis, J. Anderson, Q. Lin and Q. Wang, *Biomacromolecules*, 2009, **10**, 113-118; f) J. I. Jay, B. E. Lai, D. G. Myszk, A. Mahalingam, K. Langheinrich, D. F. Katz and P. F. Kiser, *Mol. Pharmaceut.*, 2010, **7**, 116-129; g) J. I. Jay, K. Langheinrich, M. C. Hanson, A. Mahalingam and P. F. Kiser, *Soft Matter*, 2011, **7**, 5826-5835; h) D. Roy and B. S. Sumerlin, *ACS Macro Letters*, 2012, **1**, 529-532; i) F. Kuralay, S. Sattayasamitsathit, W. Gao, A. Uygun, A. Katzenberg and J. Wang, *J. Am. Chem. Soc.*, 2012, **134**, 15217-15220; j) H. Kim, Y. J. Kang, E. S. Jeong, S. Kang and K. T. Kim, *ACS Macro Lett.*, 2012, **1**, 1194-1198; k) H. Kim, Y. J. Kang, S. Kang and K. T. Kim, *J. Am. Chem. Soc.*, 2012, **134**, 4030-4033; l) W. Wu and S. Zhou, *Macromol. Biosci.*, 2013, **64**, 1464-1477; m) Y. Li and S. Zhou, *Chem. Commun.*, 2013, **49**, 5553-5555; n) Y. Kotsuchibashi, R. V. C. Agustin, J.-Y. Lu, D. G. Hall and R. Narain, *ACS Macro Lett.*, 2013, **2**, 260-264; o) R. Ma and L. Shi, *Polym. Chem.*, 2014, **5**, 1503-1518.
- M. G. Chudzinski, Y. C. Chi and M. S. Taylor, *Aust. J. Chem.*, 2011, **64**, 1466-1469.
- W.-M. Wan, F. Cheng and F. Jäkle, *Angew Chem Int Edit*, 2014, **53**, 8934-8938.
- a) J. T. Lai, D. Filla and R. Shea, *Macromolecules*, 2002, **35**, 6754-6756; b) W. M. Wan and C. Y. Pan, *Chem. Commun.*, 2008, 5639-5641; c) W. M. Wan and C. Y. Pan, *Polym. Chem.*, 2010, **1**, 1475-1484.
- F. Cheng, E. M. Bonder and F. Jäkle, *Macromolecules*, 2012, **45**, 3078-3085.
- a) L. M. Greig, A. M. Z. Slawin, M. H. Smith and D. Philp, *Tetrahedron*, 2007, **63**, 2391-2403; b) T. Beringhelli, G. D'Alfonso, D. Donghi, D. Maggioni, P. Mercandelli and A. Sironi, *Organometallics*, 2007, **26**, 2088-2095; c) D. Maggioni, T. Beringhelli, G. D'Alfonso, M. C. Malatesta, P. Mercandelli and D. Donghi, *Z. Phys. Chem.*, 2013, **227**, 751-773; d) P. Thilagar, D. Murillo, J. W. Chen and F. Jäkle, *Dalton Trans.*, 2013, **42**, 665-670.
- a) P. X. Xing, L. S. Dong, Y. X. An, Z. L. Feng, M. Avella and E. Martuscelli, *Macromolecules*, 1997, **30**, 2726-2733; b) P. H. Tung, S. W. Kuo, S. C. Chen, C. L. Lin and F. C. Chang, *Polymer*, 2007, **48**, 3192-3200; c) C. Belabed, Z. Benabdelghani, A. Granado and A. Etxeberria, *J. Appl. Polym. Sci.*, 2012, **125**, 3811-3819; d) H. Bourara, S. Hadjout, Z. Benabdelghani and A. Etxeberria, *Polymers-Basel*, 2014, **6**, 2752-2763; e) D. P. Sweat, M. Kim, A. K. Schmitt, D. V. Perroni, C. G. Fry, M. K. Mahanthappa and P. Gopalan, *Macromolecules*, 2014, **47**, 6302-6310.
- a) Q. Bo and Y. Zhao, *J Polym Sci Pol Chem*, 2006, **44**, 1734-1744; b) H. D. Koh, J. P. Lee and J. S. Lee, *Macromol. Rapid Comm.*, 2009, **30**, 976-980; c) I. Vukovic, G. ten Brinke and K. Loos, *Macromolecules*, 2012, **45**, 9409-9418; d) S. Roland, R. E. Prud'homme and C. G. Bazuin, *ACS Macro Lett.*, 2012, **1**, 973-976; e) J. Chen, J. Duchet, D. Portinha and A. Charlot, *Langmuir*, 2014, **30**, 10740-10750.
- a) C. R. Wade, A. E. J. Broomsgrove, S. Aldridge and F. P. Gabbai, *Chem. Rev.*, 2010, **110**, 3958-3984; b) N. H. Evans and P. D. Beer, *Angew. Chem. Int. Ed.*, 2014, **53**, 11716-11754.

12. a) M. J. Fasolka and A. M. Mayes, *Ann. Rev. Mater. Res.*, 2001, **31**, 323-355; b) S. B. Darling, *Prog. Polym. Sci.*, 2007, **32**, 1152-1204; c) I. W. Hamley, *Prog. Polym. Sci.*, 2009, **34**, 1161-1210.
13. a) U. H. F. Bunz, *Adv. Mater.* 2006, **18**, 973-989; b) A. S. d. León, A. d. Campo, M. Fernández-García, J. Rodríguez-Hernández and A. Muñoz-Bonilla, *ACS Appl. Mater. Interfaces*, 2013, **5**, 3943-3951.
14. a) T. Liu, H. C. Su, X. J. Qu, P. Ju, L. Cui and S. Y. Ai, *Sensor Actuat. B-Chem.*, 2011, **160**, 1255-1261; b) P. Raghu, T. M. Reddy, K. Reddaiah, B. E. K. Swamy and M. Sreedhar, *Food. Chem.*, 2014, **142**, 188-196.
15. a) M. Kesik, F. E. Kanik, J. Turan, M. Kolb, S. Timur, M. Bahadir and L. Toppare, *Sensor Actuat. B-Chem.*, 2014, **205**, 39-49; b) F. Arduini, F. Ricci, C. S. Tuta, D. Moscone, A. Amine and G. Palleschi, *Anal. Chim. Acta*, 2006, **580**, 155-162; c) X. Sun and X. Y. Wang, *Biosens. Bioelectron.*, 2010, **25**, 2611-2614.